

# Hopf bifurcations and slow-fast cycles in a model of plankton dynamics

Isabel Fernández, José M. López, José M. Pacheco, César Rodríguez

Universidad de Las Palmas de Gran Canaria,

Departamento de Matemáticas,

Campus de Tafira, 35017 Las Palmas de Gran Canaria,

SPAIN

Tlf: +34 928 458818 ; Fax: +34 928 458811

e-mail: pacheco@dma.ulpgc.es

## Abstract

The existence of Hopf bifurcations and slow-fast cycles in the dynamics of a model for the interaction between phyto- and zooplankton is considered. A sensible and easily interpretable dimensionless version of the model is presented, followed by a numerical bifurcation analysis in a two-dimensional parameter space. The biological meaning of the parameters and qualitative features in phase space are stressed.

**Keywords:** plankton models, bifurcation analysis, slow-fast cycles

# 1 Introduction

In the open sea, plankton populations live in an ever-changing environment where equilibrium situations are the exception rather than the rule. Quite often, sudden and dramatic variations in biomass happen due to the internal mechanisms that rule the behaviour of the planktonic components.

Therefore, it is natural to look for models of plankton dynamics able to account for the onset of oscillations of various classes; among them, the slow-fast dynamics related to excitable variables is frequently observed in natural environments. There is no need of formulating complicated models: Even fairly easy ones can account for very rich dynamics.

In this paper, as in Truscott (1995), plankton is divided into only two classes, phytoplankton and zooplankton, and they stand in a prey-predator relationship. See also Steele and Henderson (1992).  $p(t)$  and  $z(t)$  shall represent the spatially averaged phyto- and zooplankton biomasses, respectively. Both classes are related to each other through grazing, by which biomass is transferred from phytoplankton to zooplankton. In the absence of grazing, the time evolution of phytoplankton is modeled by a logistic law with growth rate  $r$  and carrying capacity  $k$ :

$$p' = rp\left(1 - \frac{p}{k}\right).$$

Grazing is introduced as a Holling III interaction term:

$$-R_{\max}z\frac{p^2}{\alpha^2 + p^2};$$

this means that for large  $p$  the consumption rate of phytoplankton per unit of grazer biomass tends to a saturation value  $R_{\max}$ .  $\alpha$  is the so-called semisat-

uration constant, which is a measure of how fast the grazing term becomes asymptotically constant: The closer  $\alpha$  is to 0, the faster is  $R_{\max}$  approached. On the other hand, the dynamics of  $z$  is a linear one in the absence of phytoplankton:  $z' = -\mu z$ , and the positive grazing effect is obtained by adding the grazing term in the  $p$  dynamics times some effectivity coefficient  $\gamma$ , a parameter that can embody the delay effect of the biomass transfer from phytoplankton into zooplankton. The above considerations are summed up in the ODE model:

$$\begin{aligned} p' &= rp\left(1 - \frac{p}{k}\right) - R_{\max}z \frac{p^2}{\alpha^2 + p^2} \\ z' &= -\mu z + \gamma R_{\max}z \frac{p^2}{\alpha^2 + p^2}. \end{aligned}$$

The aims of this paper are:

- a) To present a different dimensionless version of the ODE model where parameters are easily interpreted from a biological viewpoint.
- b) To develop a bifurcation analysis leading to the understanding of the plankton dynamics through Hopf bifurcations and then to slow-fast cycles. Hopf bifurcations are one of the most employed tools in describing the onset of oscillations in many systems, ranging from mechanical to biological to social ones. See Fernández and Pacheco (2001); Pacheco et al. (1997).
- c) To obtain further insight of the biological interpretations of the model.

## 2 Qualitative analysis of the model

### 2.1 Adimensionalization

Obtaining dimensionless forms for the equations is a primary task before embarking on further analyses in any model study. As a rule, equations can be

written in simpler forms, the number of parameters is reduced, and the remaining ones are found to be easily interpretable combinations of the original ones. The procedure is not unique and usually units must be carefully chosen. A most interesting discussion can be found in Fowler (1997), the standard technique is explained in Edelstein-Keshet (1988), and many interesting examples are described in Murray (1989).

In this case a nice dimensionless version of the model can be obtained by scaling the variables

$$t = t^* \bar{t}, \quad p = p^* \bar{p}, \quad z = z^* \bar{z}$$

with the new units:

$$\bar{t} = \frac{1}{r}, \quad \bar{p} = k, \quad \bar{z} = \frac{r}{R_{\max}} k.$$

This choice is different from the one proposed in Truscott (1995), and amounts to using the linear relaxation time and the carrying capacity of phytoplankton as new time and phytoplankton biomass units. The zooplankton biomass unit is simply the fixed fraction of  $k$  given by the dimensionless quotient  $\frac{r}{R_{\max}}$  relating the linear growth rate of phytoplankton and the maximum consumption rate per unit grazer. By plugging these values into the equations and dropping the asterisks of the new variables, the model is written in the simpler form:

$$p' = p(1 - p) - z \frac{p^2}{\nu^2 + p^2}$$

$$z' = \beta \left[ \frac{p^2}{\nu^2 + p^2} - \omega \right] z.$$

The original six constants are reduced to only three non-dimensional ones:

$$\nu = \frac{\alpha}{k}, \quad \delta = \frac{\mu}{r}, \quad \text{and} \quad \beta = \frac{R_{\max}}{r} \gamma,$$

$$\nu = \frac{\alpha}{k}, \delta = \frac{\mu}{r}, \text{ and } \beta = \frac{R_{\max}}{r}\gamma,$$

where  $\nu = \frac{\alpha}{k}$  expresses the semisaturation constant  $\alpha$  as a fraction of the carrying capacity  $k$ ,  $\delta = \frac{\mu}{r}$  is the quotient of the linear growth rates of both species, and  $\beta = \frac{R_{\max}}{r}\gamma$  is the analogue of  $\gamma$ —note that the factor is the inverse fraction of the one used to define the zooplankton unit. Actually,  $\beta$  plays no role in the analyses to follow; instead, the dimensionless combination  $\omega = \frac{\delta}{\beta}$  is introduced for the sake of simplicity, notational convenience, and interpretability. It is interesting to observe that  $\omega$  measures how large the linear decay rate  $\mu$  of zooplankton is with respect to the maximum rate  $\gamma R_{\max}$  of zooplankton biomass creation out of phytoplankton. This remark will often be used in the sequel.

## 2.2 Singular points and their stability

For any initial condition  $(p_0, z_0)$  in the first orthant of the phase plane, the corresponding orbit never leaves it, for it follows from the model construction that both the  $p$ -axis and the  $z$ -axis are trajectories of the system. The analysis is therefore restricted to this area.

The manifold  $z' = 0$  is the union of the  $p$ -axis and the line

$$p = \nu \sqrt{\frac{\omega}{1-\omega}},$$

while the  $p' = 0$  manifold is formed by the  $z$ -axis and the curve, asymptotic to the  $z$ -axis when  $p \rightarrow 0$ , defined by the equation

$$z = \frac{(1-p)(\nu^2 + p^2)}{p}.$$

The above equations show immediately that two conditions must be fulfilled for the system to have a singular point interior to the first orthant:

$$\omega < 1 \text{ and } p < 1$$

the other only two singular points being  $(0,0)$  and  $(1,0)$  for any choice of the parameter values. Note also the equivalence

$$p < 1 \iff \nu < \sqrt{\frac{1}{\omega} - 1}.$$

It is straightforward to show that  $(0,0)$  is a saddle point whose stable and unstable manifolds are the  $z$ -axis and the  $p$ -axis respectively. The point  $(1,0)$  is also a saddle point with the  $p$ -axis as stable manifold –stated simply, this means that the restricted dynamics is given by a logistic–, while the unstable manifold is locally given by the curve  $z = (1-p)(\nu^2 + p^2)/p$ .

Once the two conditions  $\omega < 1$  and  $p < 1$  are met, the singular point

$$(p^*(\omega, \nu), z^*(\omega, \nu)) = \left( \nu \sqrt{\frac{\omega}{1-\omega}}, \frac{\nu}{\omega} \left[ 1 - \nu \sqrt{\frac{\omega}{1-\omega}} \right] \right)$$

in the interior of the first orthant is the unique intersection point of the curves (Figure 1):

$$p = \nu \sqrt{\frac{\omega}{1-\omega}}$$

$$z = \frac{(1-p)(\nu^2 + p^2)}{p}$$

The relationship between  $\nu$  and  $\omega$  governs the stability of this singular point, and in case there should exist an stability shift for some pair(s)  $(\omega, \nu)$ , a bifurcation problem must be considered. This is the aim of the next section.

## 2.3 A bifurcation analysis

### 2.3.1 The shape of the $p' = 0$ manifold

From a geometric viewpoint the stability of the singular point depends on the shape of the curved component of the  $p' = 0$  manifold, the curve

$$z = \frac{(1-p)(\nu^2 + p^2)}{p}.$$

Its slope  $-\frac{\nu^2 + p^2}{p^2} + 2(1-p)$  depends (Figure 2) on the parameter  $\nu$ . For large  $\nu$  the slope is always negative and the curve descends monotonically from  $+\infty$  to 0 along the interval  $(0, 1]$ . This is easily proved: Writing

$$-\frac{\nu^2 + p^2}{p^2} + 2(1-p) = 1 - 2p - \frac{\nu^2}{p^2} < 0$$

in the form  $2p + \frac{\nu^2}{p^2} > 1$ , it follows trivially that it suffices to take  $\nu$  large enough for the inequality to hold. To quantify how large  $\nu$  must be, consider that the minimum  $m$  of the expression  $2p + \frac{\nu^2}{p^2}$  occurs when  $p_m$  satisfies  $2 - 2\frac{\nu^2}{p_m^3} = 0$ , or equivalently  $p_m = \nu^{2/3}$ . Therefore  $m > 1$  if  $2\nu^{2/3} + \frac{\nu^2}{\nu^{4/3}} = 3\nu^{2/3} > 1$ , or  $\nu > \nu_{crit} = \sqrt{\frac{1}{27}} = 0.19245\dots$

For  $\nu < \nu_{crit}$ , two extrema –a minimum and a maximum– appear at the values  $p_{min}$  and  $p_{max}$ , with  $0 < p_{min} < p_{max} < 1$ . Therefore the slope of the curve is positive in the interval  $(p_{min}, p_{max})$ , its graph shows a characteristic hump form, and the linear stability analysis of the point  $(p^*, z^*)$  depends on whether  $p^* \in (p_{min}, p_{max})$  or not. To see when this is the case, write:

$$p_{min} < p^* = \nu \sqrt{\frac{\omega}{1-\omega}} < p_{max}$$

to obtain the following estimates for  $\omega$ :

$$\begin{aligned} \left(\frac{p_{min}}{\nu}\right)^2 < \frac{\omega}{1-\omega} < \left(\frac{p_{max}}{\nu}\right)^2 &\iff \\ \iff \frac{\left(\frac{p_{max}}{\nu}\right)^2}{1 + \left(\frac{p_{max}}{\nu}\right)^2} > \omega > \frac{\left(\frac{p_{min}}{\nu}\right)^2}{1 + \left(\frac{p_{min}}{\nu}\right)^2} \end{aligned}$$

that must be satisfied (remember that  $\nu < \nu_{crit}$ ) for the singular point  $(p^*, z^*)$  to be in the “uphill” part of the hump, to the left of the maximum. When this is the case, an annular closed region around the singular point can be determined

in phase space such that any orbit entering it will remain there forever, so the Poincaré-Bendixson theorem is applied and a limit cycle exists. See Arrowsmith and Place (1994); Verhulst (1990).

### 2.3.2 Numerical analyses in the $(\omega, \nu)$ plane

The model dynamics depends essentially on the two parameters  $\omega$  and  $\nu$ , and the bifurcation analysis amounts to study those sets of pairs  $(\omega, \nu)$  for which the qualitative aspect of the phase portrait is the same. In this model no simple expressions for  $p_{\min}$  and  $p_{\max}$  can be obtained for general  $\nu$ , so the following step will be the numerical analysis of some geometrical shapes in the  $(\omega, \nu)$  plane.

Remember that the conditions for the existence of a singular point in the first orthant amount to

$$\omega < 1 \text{ and } \nu < \sqrt{\frac{1}{\omega} - 1}$$

so the set of feasible pairs in the  $(\omega, \nu)$  plane is the open set  $\Omega$  limited by the positive  $\omega$ -axis, the positive  $\nu$ -axis and the graph of  $\nu = \sqrt{\frac{1}{\omega} - 1}$  (Figure 3).

By establishing a grid over  $\Omega$  and computing the eigenvalues  $\lambda(\omega, \nu)$  of the jacobian matrix at the grid points, the transition from two negative real eigenvalues to negative real part complex ones, and from these to positive real part complex ones can be tracked across two parabola-like curves that can be determined by fitting adequate trigonometric polynomials to the observed points. This procedure can be easily programmed in Mathematica or Maple.

Therefore,  $\Omega$  is union of three open regions and the two parabola-like curves separating them<sup>1</sup>,  $\Gamma_{N-S}$  and  $\Gamma_{S-H}$ .  $\Gamma_{N-S}$  runs from the origin to  $(1, 0)$  with

<sup>1</sup>Here  $N$  means “node”,  $S$ , “spiral”, and  $H$ , “Hopf”.



a single maximum at (0.4, 0.8);  $\Gamma_{S-H}$  runs from (0.5, 0) to (1, 0) and its single maximum is at (0.75, 0.19). The three open regions are (Figure 4):

$\Omega_N$ , above  $\Gamma_{S-H}$ : For  $(\omega, \nu)$  in this region,  $(p^*, z^*)$  is a stable node (two negative real eigenvalues) whose attraction basin is the interior of the first orthant.

$\Omega_S$ , limited by both  $\Gamma_{N-S}$ ,  $\Gamma_{S-H}$ , and the  $\omega$ -axis: For  $(\omega, \nu)$  in this region,  $(p^*, z^*)$  is a stable spiral point (negative real part of the complex eigenvalues) and, again, the attraction basin is the interior of the first orthant. If  $(p^*, z^*) \in \Gamma_{N-S}$ , it behaves as a degenerate node.

$\Omega_H$ , below  $\Gamma_{S-H}$ : For  $(\omega, \nu)$  in this region,  $(p^*, z^*)$  is a unstable spiral point surrounded by a stable limit cycle. Then,  $\Gamma_{S-H}$  is the bifurcation set of a transcritical Hopf bifurcation: When crossing it, the stable spiral point  $(p^*, z^*)$  splits into an unstable spiral point and a stable limit cycle surrounding it. The attraction basin is the interior of the first orthant as well. Numerical computations show that the Hopf bifurcation condition (see Arrowsmith and Place (1994))

$$\left[ \frac{\partial(\operatorname{Re} \lambda(\omega, \nu))}{\partial \bar{\mathbf{n}}} \right]_{\Gamma_{S-H}} > 0$$

is also met.

### 3 Biological interpretation

To obtain a sensible explanation in biological terms of the above discussion the definition and interpretation of the parameters  $\omega$  and  $\nu$  must be remembered:

$$\omega = \frac{\delta}{\beta} = \frac{\mu}{\gamma R_{\max}}, \nu = \frac{\alpha}{k}$$

$\omega$  expresses the relationship between the linear decay rate  $\mu$  of zooplankton and the maximum rate  $\gamma R_{\max}$  of zooplankton biomass creation out of phytoplankton.  $\nu$  indicates how fast the maximum grazing rate is approached: Actually, it is a measure of how much phytoplankton is needed for grazers to reach a satiated state. Small values indicate rapid satiation, while larger values are the signal of a harder struggle for existence.

Given that for the existence of  $(p^*, z^*)$  it is required that  $\omega < 1$ , *i.e.*  $\mu < \gamma R_{\max}$ , small values of  $\omega$  mean that the nonlinear “birth” rate  $\gamma R_{\max}$  is much larger than the linear decay rate  $\mu$ . Therefore, if  $\nu$  is small, *i.e.* the maximum grazing rate  $R_{\max}$  is rapidly approached, the net balance is positive for zooplankton growth. It must be noted that for large  $\nu$  the interval of feasible  $\omega$  values becomes small quite rapidly: For instance, when  $\nu = 1$  the interval is  $(0, 1/2)$ . Should any  $\omega > 1/2$  be chosen, the model dynamics shows that the populations  $(p, z) \rightarrow (1, 0)$ , that is, zooplankton disappears as phytoplankton settles comfortably at its carrying capacity.

Summing up, the biology underlying the model is characterized by the conflict between “ $\nu$ , or how much phytoplankton is needed for grazers to reach a satiated state” and “ $\omega$ , or how efficient is zooplankton in the transformation of phytoplankton biomass into its own biomass”. This is reflected in the following, purely qualitative table:

$\nu \backslash \omega$	small	large
small	Stable populations	Cyclic behaviour
large	Stable populations	Zooplankton extinction

It must be observed that the analysis in 2.3.2 shows that stable populations may be approached either directly (stable nodes) or after decaying oscillations (stable spiral points).

## 4 Slow-fast cycles

Roughly speaking, a slow-fast cycle is a cycle along which the travelling speed of one state variable is dramatically altered on some parts of the cycle, and this variable is called a “fast” variable. The other state variable is the “slow” one. The graph of the time evolution of the fast variable shows a typical oscillatory pattern: A wave train of steep humps with more slowly decreasing lees (Figure 5).

Inspection of the relative position of the  $p' = 0$  and  $z' = 0$  manifolds reveals a slow-fast cycle situation if one of them –the one corresponding to the fast variable– is an  $S$ -shaped curve and the other one crosses it transversally through some point in the central part of the  $S$ . This is exactly the case of the model for  $(\omega, \nu) \in \Omega_H$ : To see it, just rotate the phase plane by an angle of  $\pi/2$  around the origin to “discover” the  $S$ -shapedness of the  $p' = 0$  manifold and how the straight line  $z' = 0$  goes across it. In this case  $p$  is the fast variable.

A slow-fast cycle will typically show  $(p, z)$  travelling counterclockwise along  $p' = 0$  (the curve  $z = (1 - p)(\nu^2 + p^2)/p$ ) up to  $(p_{\max}, z_{\max})$ , then jumping horizontally to the descending part of the same curve, then descending to the point  $(p_{\min}, z_{\min})$ , where a new horizontal track is traversed, and so on (Figure 6). See Verhulst (1990).

According to the Hopf bifurcation theorem, the amplitude of the limit cycle created when an stable spiral points splits into an unstable one and a stable

cycle grows as the pair of bifurcation parameters  $(\omega, \nu)$  crosses transversally the bifurcation set  $\Gamma_{S-H}$  into the region  $\Omega_H$ . Therefore, any sensible analysis will track the parameter values  $(\omega, \nu) \in \Omega_H$  in such a way that the gradient of the amplitude is maximum. The numerical experiments show that this is the case for the right corner of  $\Omega_H$ ; this means that  $\nu$  must be small –grazers are soon satiated– and  $\omega$  rather large –the nonlinear rate  $\gamma R_{\max}$  is smaller than the linear decay rate  $\mu$ .

## 5 Conclusions and views

The model considered in this paper stresses the role of various relationships when interpreted from a biological viewpoint and accounts for several interesting features of plankton dynamics.

$\nu$  –or its dimensional counterpart  $\alpha$ – controls how fast predators, *i. e.* zooplankton, are satiated: Small values of the parameter correspond with fast satiation. From the Oceanography viewpoint, a small  $\nu$  can correspond to a stage where phytoplankton biomass grows quickly: a so-called “algal bloom”. The other interesting parameter is  $\omega$ , it is a measure of the relative importance of the linear decay rate of zooplankton and the maximum nonlinear rate of zooplankton biomass creation out of phytoplankton. Both parameters span a two-dimensional space where a feasible subset  $\Omega$  of parameter pairs is obtained. Moreover, there exists a bifurcation set –the curve  $\Gamma_{S-H}$ – separating stable spiral behaviour from unstable spiral behaviour and a stable limit cycle.

Therefore the Hopf bifurcation is a characteristic feature of this model meaning that for small values of  $\nu$  and rather large values of  $\omega$  plankton can develop stable oscillating patterns out of any initial distribution of phyto- and zoo-

plankton. If  $\nu$  is very small and  $\omega \approx 1$ , the stable cycle shows a typical slow-fast behaviour. Informally, this means that when predators are rapidly satiated and their efficiency in transforming prey into predator biomass is not large enough to balance the linear decay, sudden and dramatic changes can occur to both components of the planktonic system. These results agree with the general conclusions of Truscott (1995), exception made of the Hopf bifurcation stage.

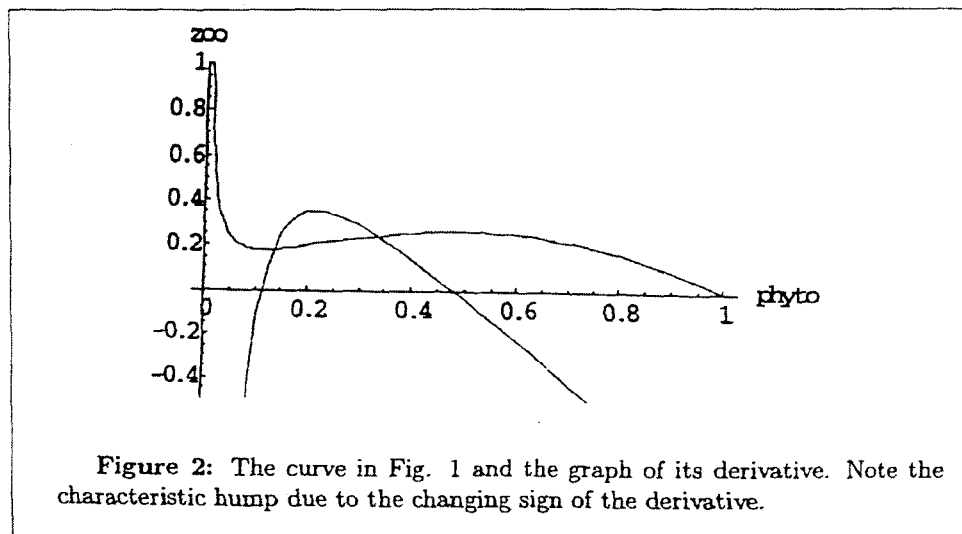
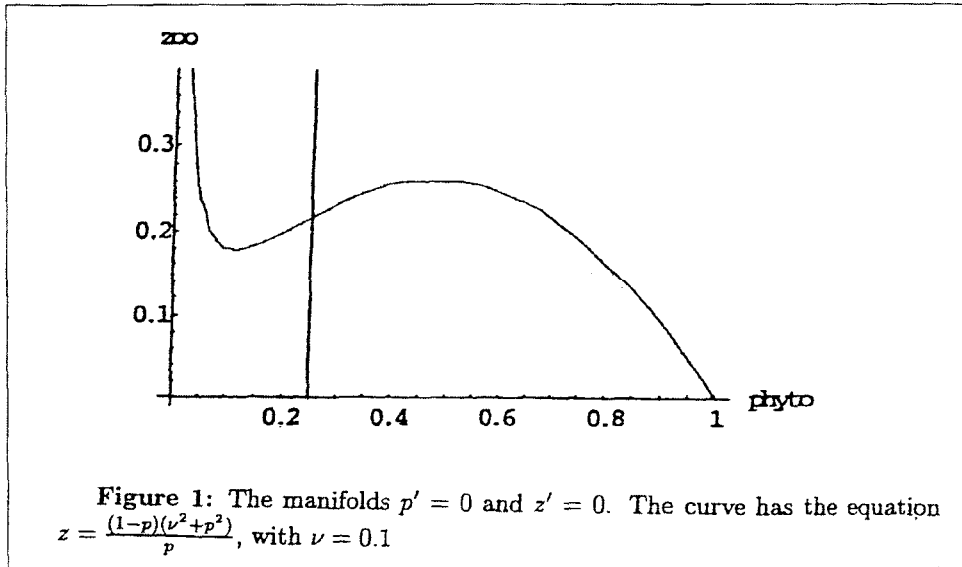
An interesting point for further study is the introduction of periodic behaviour in some of the model parameters. Periodic upwellings controlled by variations in the depth of the thermocline –as in the EN phase of ENSO– can be represented by a modulation like  $\nu = \nu(t)$  with  $\nu(t) = \nu(t + T)$ , where the “only” difficulty is the determination of the period  $T$ . See Fernández and Pacheco (2000) and references therein. In addition to that, upwellings usually imply the appearance of predators external to the planktonic systems –fish– that can highly modify the dynamics and due to their mobility make it necessary, as in Malchow (1994), to consider spatial distribution effects as well.

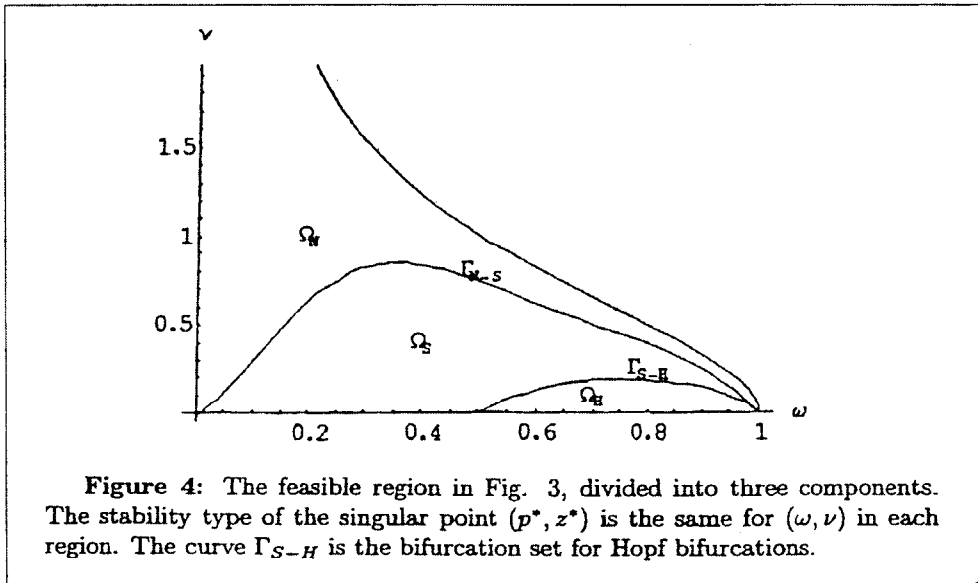
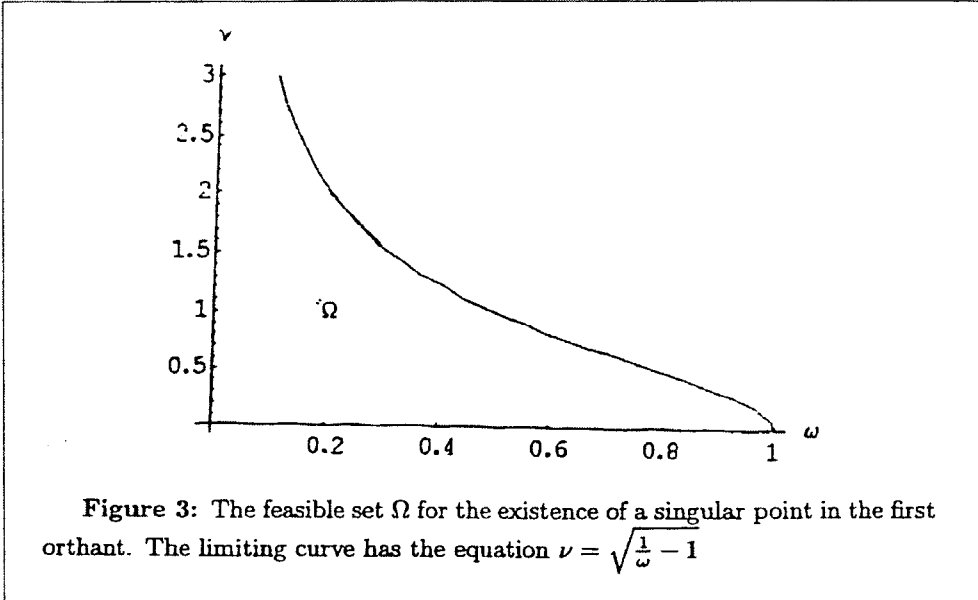
## References

- [1] Arrowsmith, D. and Place, C., 1994. An introduction to dynamical systems, Cambridge UP, Cambridge, 423 pp.
- [2] Edelstein-Keshet, L., 1988. Mathematical models in biology. Random House-Birkhäuser, New York, 586 pp.
- [3] Fernández, I. and Pacheco, J., 2000. Bases para la predicción de ENSO. In: R. García and E. Hernández (Editors), El Niño: Climatología, efectos y predicción, Universidad Complutense-Mapfre, Madrid, pp. 93-132.

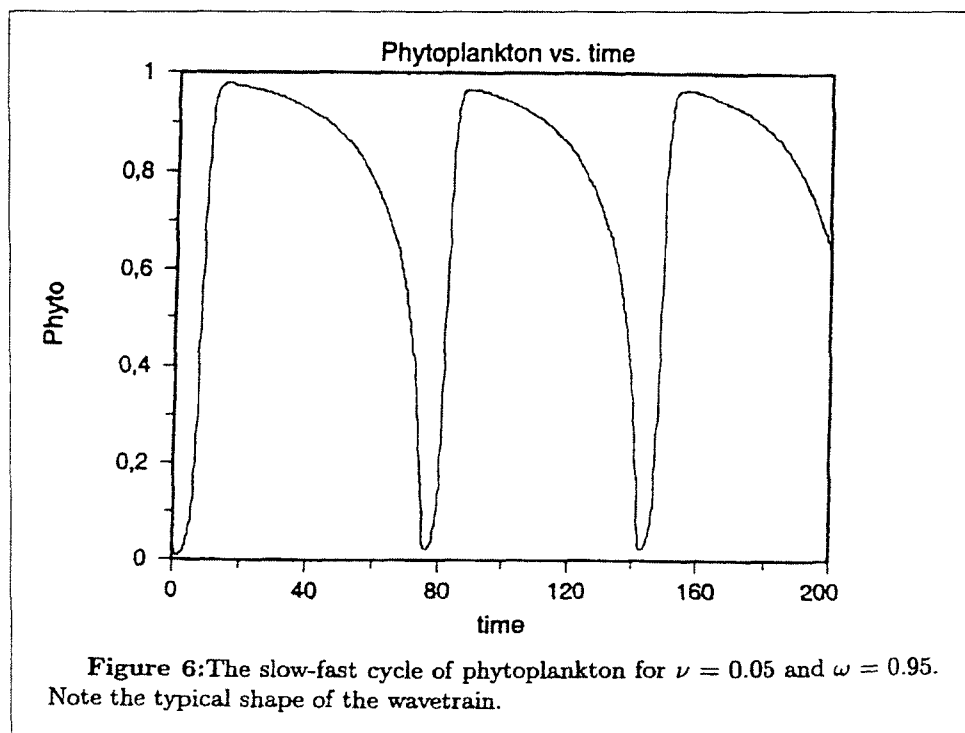
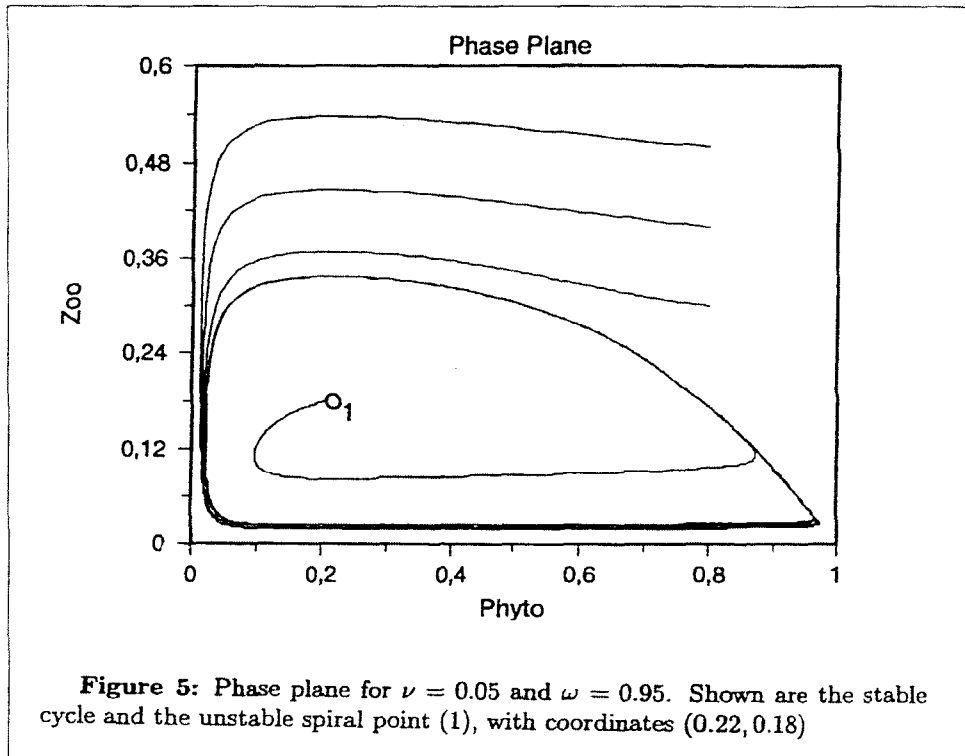
- [4] Fernández. I. and Pacheco, J., 2001. Some mathematical aspects in the modelling of environmental quality. In: M. Matthies (Editor), *Integrative approaches to natural and social dynamics*, Springer Verlag, Berlin, pp. 235-248.
- [5] Fowler, A.,1997. *Mathematical models in the applied sciences*. Cambridge Univ. Press, Cambridge, 402 pp.
- [6] Malchow, H., 1994. Non-equilibrium structures in plankton dynamics, *Ecol. Modelling*, 75: 123-134.
- [7] Murray, J.,1989. *Mathematical biology*. Springer Verlag, New York, 767 pp.
- [8] Pacheco, J., Rodríguez, C. and Fernández, I.,1997. Hopf bifurcations in a predator-prey model with social predator behaviour, *Ecol. Modelling*, 105: 83-87.
- [9] Steele, J. and Henderson, W., 1992. The role of predation in plankton models, *J. Plankton Res.*, 14(1): 157-172.
- [10] Truscott, J. E.,1995. Environmental forcing of simple plankton models, *J. Plankton Res.*, 17(12): 2207-2232.
- [11] Verhulst, F.,1990. *Nonlinear differential equations and dynamical systems*. Springer Verlag, Berlin, 277 pp.

## FIGURES









## ÍNDICE

	<u>Págs.</u>
PRESENTACIÓN .....	5
<i>SECCIÓN MATEMÁTICAS</i>	
M.N. MUKHERJEE, B. ROY & P. SINHA. Concerning $p$ -closed Topological Spaces .....	9
H.M. SRIVASTAVA. Some Integral Representations for the Jacobi and Related Hypergeometric Polynomials .....	25
M. SÁNCHEZ GARCÍA & M.I. SOBRÓN FERNÁNDEZ. Cálculo de probabilidades de consistencia y paternidad en sistemas genéticos: estudios de dos modelos .....	35
J.J. PRIETO MARTÍNEZ. Estimación no paramétrica del número de especies en un ecosistema de tamaño desconocido via estimadores Jackknife generalizados en poblaciones finitas .....	47
B. BONILLA, M. RIVERO, L. RODRÍGUEZ-GERMÁN, J.J. TRUJILLO, A.A. KILBAS & N.G. KLIMETS. Mittag-Leffler Integral Transform on $L_v$ $\gamma$ -spaces .....	65
B.B. WAPHARE. Real Inversion Formula for the Distributional Generalized Meijer Transformation .....	79
M.C. MUKHERJEE. On Partial Semi Bilinear Generating Function Involving Hypergeometric Polynomial - I .....	93
R.K. SAXENA, J. RAM & S.L. KALLA. Unified Fractional Formulas for the Generalized H-function .....	97
R.K. SAXENA, C. RAM & S.L. KALLA. Applications of Generalized H-function in Bivariate Distributions .....	111
I. FERNÁNDEZ, J.M. LÓPEZ, J.M. PACHECO & C. RODRÍGUEZ. Hopf Bifurcations and Slow-fast Cycles in a Model of Plankton Dynamics .....	121
<i>HISTORIA Y FILOSOFÍA DE LA CIENCIA</i>	
C. ROMO SANTOS. Aproximación a los fondos matemáticos de judaica y de hebraica de la Biblioteca Nacional de Madrid .....	141
N. HAYEK. Una biografía de Abel .....	147
<i>DIVULGACIÓN CIENTÍFICA</i>	
N. HAYEK. El conjunto de Mandelbrot .....	169
<i>VIDA ACADÉMICA</i>	
Memoria de actividades realizadas durante el año 2002 .....	207
<b>IN MEMORIAM:</b> Excmo. Sr. Dr. D. Antonio González González .....	209
<b>INSTRUCCIONES PARA LOS AUTORES</b> .....	227
<b>INSTRUCTIONS TO THE AUTHORS</b> .....	229